ELSEVIER

Composites: Part A 33 (2002) 301–314

composites
Part A: applied science and manufacturing

www.elsevier.com/locate/compositesa

Optimal post-manufacturing cooling paths for thermoplastic composites

Fazıl O. Sonmez*, Erhan Eyol

Department of Mechanical Engineering, Bogazici University, Istanbul, Bebek 80815, Turkey

Received 27 November 2000; revised 13 August 2001; accepted 11 September 2001

Abstract

The objective of this study is to determine the optimal cooling scheme to minimise the processing time during the cooling stage in press moulding. The optimisation is subject to the quality constraints concerning maximum allowable residual stress and recommended levels of crystallinity. Since they depend on temperature state, a one-dimensional transient heat transfer analysis was carried out using a finite difference method so as to obtain the transient temperature profile through the thickness of the laminate. The heat transfer analysis was then coupled with a crystallisation-kinetics model. Using a plane-strain viscoelastic model, residual stress distribution was obtained corresponding to a given cooling scheme. These models were then integrated into an optimisation algorithm called sequential simplex, to minimise the cooling time without compromising quality requirements. Significant reduction in processing time was obtained for APC-2 laminates.

Keywords: A. Laminates; B. Residual stresses; E. Compression moulding; Finite element analysis (FEA)

1. Introduction

Press moulding is a widely used technique to fabricate thermoplastic–matrix–composite laminates. This is achieved by placing the plies with proper sequence into a mould cavity having the desired shape, and heating up. By keeping the material under pressure at temperatures higher than the melting point of the thermoplastic, intimate contact is achieved and molecular diffusion between individual plies is allowed to take place. Consequently, bulk properties are restored at their interfaces. Finally, the composite is cooled down to the room temperature. An illustration of the press moulding process can be seen in Fig. 1.

Many thermoplastic composite laminates, such as those made of APC-2, undergo a considerable temperature drop during their post-manufacturing cool-down because of their high melting points. This thermal excursion induces significant residual thermal stresses in laminated composite structures as an unavoidable consequence of the large difference in thermal expansion coefficients of fibre and polymeric matrix. For a typical carbon-reinforced thermoplastic composite, while temperature increase induces significant expansion of the laminate in the transverse direction but almost none along the fibre direction. Besides, fibres being themselves anisotropic contribute to this effect. Anisotropy is especially effective in cross lay-ups, where fibres run in different directions in different layers. Existence of temperature gradients through the thickness of the laminate during cooling is also a factor in residual stress development. This is because of the dependence of the mechanical properties on temperature. When different parts of the laminate experience different temperature histories, their deformation behaviour will also be different. Discrepancy in the deformation response naturally results in the development of residual stresses.

Residual stresses can have significant detrimental effects on the performance of composite structures by causing fibre buckling or void formation during solidification, reducing strength and initiating transverse cracks or delaminations [1,2]. These stresses can be as high as the ultimate transverse strength of the composite. Therefore, residual thermal stresses should be within tolerable limits to ensure the desired performance and reliability of the composite structures during service.

Productivity of a manufacturing process decides its feasibility. Higher productivity can be achieved by reducing the process time. However, the quality of the final product must be satisfactory as well. One of the indications of quality is the residual stress level. Another is the crystallinity of the matrix. During processing of semicrystalline thermoplastic–matrix composites, crystallisation occurs above the glass transition temperature as the laminate cools down from

* Corresponding author. Tel.: +90-212-358-1540/2196; fax: +90-212-287-2456.

E-mail address: sonmezfa@boun.edu.tr (F.O. Sonmez).

1359-835X/02/$ - see front matter
PII: S1359-835X(01)00133-6

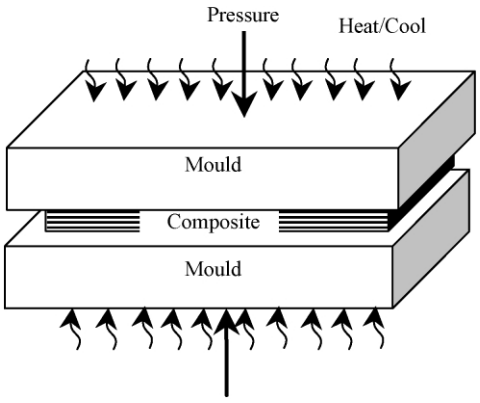

Fig. 1. Illustration of the press moulding process.

the melted state. Mechanical properties such as strength, fatigue and impact resistance are influenced by crystallisation [3–11]. Slow cooling results in high crystallinity, which leads to a brittle and higher modulus polymer. In contrast, fast-cooled polymers have lower modulus, lower strength, but higher toughness due to low crystallinity. Therefore, one should ensure a crystallinity level that will yield desired properties in the final product.

The aim of this study is to develop an optimisation scheme to determine the optimal cooling path so that a thermoplastic composite laminate can be produced by press moulding in a minimum time without leading to excessive residual stresses and non-optimal crystallinity levels.

A number of researches studied different aspects of the problem through experimental, analytical or numerical methods. Unger and Hansen [12] investigated the effect of cooling rate on residual stress development in APC-2 while cooling from the molten state by measuring the radius of curvature developed in unsymmetrical laminates. They also studied the effect of annealing temperature by heating from the amorphous state. They concluded that control of the matrix properties and stress state through cooling rate or annealing allows the material response of APC-2 to be optimised. A process of quench cooling followed by an anneal cycle to a specified temperature was identified as one such method effective in minimising residual stresses. Gurtin and Murphy [13] attempted to obtain optimal cooling paths to minimise residual stresses by employing a linear thermoviscoelastic approach. They considered a thin, isotropic, thermorheologically simple, linearly viscoelastic plate reinforced by a random system of fibres lying in the plane of the plate. For a Maxwell material, they solved the Euler's equation in closed form and they used this equation to compute the optimal temperature path for polymethyl methacrylate cooling from 90 to 80°C. The cooling time was 5 h. They used a constant thermal expansion coefficient in their analysis. Weitsman [14] presented an analytical scheme to find the optimal temperature path that minimises residual thermal stresses in thermorheologically simple linear viscoelastic thin plates. The optimal temperature paths were smooth and continuous during all intermediate temperatures, but discontinuous at initial and final times. Later, Weitsman and Harper [15] obtained results for the optimal cooling of symmetric and balanced cross-ply laminates and adhesive joints using an optimisation scheme based on the one developed in Ref. [14] and recent data on viscoelastic response of graphite/epoxy composites. As in Ref. [14], cooling paths possessed discontinuities at the initial and final times. In all the cases investigated, cooling paths undershot the final temperature and required an upward jump at the final time. Harper [16] used an analytical method similar to those developed in Refs. [13,14] for predicting optimal cooling paths minimising residual stresses. In this case, thermoviscoelastic behaviour of the plate material was modelled by employing both horizontal and vertical shift factors. Lee and Weitsman [17] obtained optimal cool-down paths to minimise residual stresses in APC-2 laminates where the response of APC-2 laminates was formulated by CLT (Classical Laminate Theory). The non-linear viscoelastic behaviour of the laminate was accounted for by means of a quasi-elastic/viscoelastic approximation. The optimal cool-down paths were found numerically by solving an integrodifferential equation iteratively. Weitsman and Zhu [18] demonstrated that it was possible to obtain an optimal temperature–time cooling path in the case of rate-dependent plastic response.

In all these studies, however, temperature was assumed to be uniform across the thickness of the plate at a given time; therefore the effect of temperature gradients induced during cooling was not taken into account. As another shortcoming regarding the previous studies, optimal cooling paths contained sudden drops and sharp decreases in temperature so that it is impossible to deliver the prescribed cooling by an instrument. They also did not include crystallisation in their optimisation scheme. For this reason, it was not possible by the previous methods to ensure that the final crystallinity was within the recommended range. Our goal in this study is to develop an optimisation scheme that also considers the above-mentioned points that were left out in previous studies. Also instead of minimising residual stresses, we chose the cooling time as our objective function to be minimised. Maximum allowable residual stress and recommended crystallinity levels, on the other hand, serve as quality constraints during the optimisation process.

2. Heat transfer analysis

A transient analysis is needed to determine the variation of temperature through the thickness of the laminate during cooling.

2.1. Assumptions and boundary conditions

The in-plane dimensions of the plate were assumed to be much greater than the thickness, h. Consequently, heat transfer through the edges can be neglected in comparison

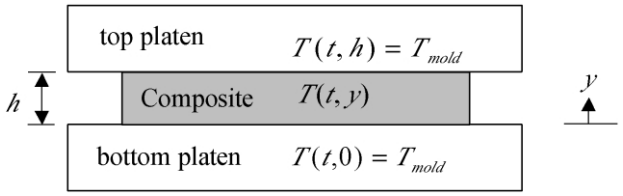

Fig. 2. The thermal boundary conditions.

to the top and bottom surfaces of the composite. A one-dimensional thermal analysis may then be assumed to yield accurate results.

The surface of the thermoplastic laminate is cooled by conduction heat transfer through the walls of the mould, which in turn are convectively cooled by a cooling fluid flowing through the press platens. We assume that the mould temperature can be reduced in a controlled manner. Considering that the mould is large and made of a highly conductive material, it acts like a heat sink having almost uniform temperature. Accordingly, the control volume to be analysed can be taken to be limited to the composite, and the temperature of the laminate at its top and bottom can be assumed to be equal to the mould temperature. Therefore,

$$T(t.0) = T_{\text{mold}} \qquad T(t,h) = T_{\text{mold}} \tag{1}$$

where T_{mold} is the temperature of the mould. The boundary conditions of the problem and the coordinate system are shown on a schematic of press mould in Fig. 2.

2.2. Initial condition

We assume that the consolidation time during which the material is kept in the molten state is sufficiently long so that steady state is reached. Therefore, at the onset of cooling, the temperature is assumed to be uniform within the mould and equal to the consolidation temperature. So,

$$T(0,y) = T_{\text{c}} \tag{2}$$

where T_{c} is the consolidation temperature.

2.3. Governing equation

For one-dimensional heat transfer, the heat conduction equation reduces to:

$$\rho C \frac{\partial T}{\partial t} = \frac{\partial}{\partial y}\left[k \frac{\partial T}{\partial y}\right] + \rho \dot{q} \tag{3}$$

where ρ is the density, C is the specific heat, k is the thermal conductivity of the composite in the transverse direction, and $\dot{q}$ is the heat generation per unit mass resulting from crystallisation. Since the effect of crystallisation on temperature is small as some previous studies [12,19] have shown, the $\dot{q}$ term in Eq. (3) is dropped in our study.

2.4. Finite difference formulation

The governing differential equation and the boundary conditions can be approximated by expressing derivatives in time and space by difference formulas. The analysed region is divided into a mesh of nodes separated by distance Δy and finite difference equations are formed at each node at finite time increments Δt to obtain temperature distribution at each time step. Two nodes are used in each ply. Therefore, Δy is equal to the half of ply thickness. Derivation of the finite difference equation for transient heat transfer through a plate, governed by Eq. (3), at node j, $y + y_j$, and time step $n + 1$, $t = t_{n+1}$, reveals [20]

$$\frac{T_j^{n+1} - T_j^n}{\Delta t} = \frac{\alpha}{2}\left[\frac{T_{j-1}^{n+1} - 2T_j^{n+1} + T_{j+1}^{n+1}}{(\Delta y)^2} + \frac{T_{j-1}^{n} - 2T_j^{n} + T_{j+1}^{n}}{(\Delta y)^2}\right] \tag{4a}$$

where

$$\alpha = \frac{k^n}{\rho^n C^n} = \text{thermal diffusivity} \tag{4b}$$

Because high performance engineering thermoplastics have very high melting points (340°C for APC-2), temperature drop during cooling is drastic. Therefore, temperature dependence of the material properties may not be neglected through using average values for the material properties in the above equation. Accordingly, the values of k, ρ and C in Eq. (4b), are updated at each time step. In order to obtain accurate results, the time step Δt was set to a sufficiently low value. The Crank–Nicolson method was used for solving the above-stated one-dimensional transient conduction problem.

3. Crystallisation model

The general Avrami theory of phase change [21], when applied to isothermal crystallisation of semi-crystalline polymers, yields the following equation:

$$\frac{c_{\text{v}}(t)}{c_{\text{v}}^{\infty}} = 1 - \exp\left[-kt^n\right] \tag{5}$$

where $c_{\text{v}}(t)$ is the volume fraction of crystallinity at time t, c_{v}^{∞} is the volume fraction of crystallinity at infinite time. The Avrami equation can be extended to nonisothermal crystallisation kinetics. An expression for nonisothermal crystallisation kinetics was proposed by Kamal and Chu [22]:

$$\frac{c_{\text{v}}(t)}{c_{\text{v}}^{\infty}} = 1 - \exp\left[-\left(\int_0^t k(t) n t^{n-1} \mathrm{d}t\right)\right] \tag{6}$$

Eq. (6) was applied to bimodal nonisothermal crystallisation of PEEK polymer and its carbon-fibre-reinforced composites by Velisaris and Seferis [23,24] and later by Cebe

[25,26]:

$$\frac{c_v(t)}{c_v^{\infty}} = w_1\left(1 - \exp\left[-\left(\int_0^t k_1 n_1 t^{n_1-1}\mathrm{d}t\right)\right]\right) + w_2\left(1 - \exp\left[-\left(\int_0^t k_2 n_2 t^{n_2-1}\mathrm{d}t\right)\right]\right) \quad (7)$$

or

$$c_v(t)/c_v^{\infty} = w_1 F_{vc1} + w_2 F_{vc2} \quad (8)$$

where w_i are the weight factors for the dual mechanism with $w_1 + w_2 = 1$ and F_{vci} is the normalised volume fraction of crystallinity corresponding to the i-th mechanism defined for non-isothermal crystallisation as:

$$F_{vci} = 1 - \exp\left[-\int_0^t K_i(t) n_i t^{(n_i-1)}\mathrm{d}t\right] \qquad i = 1,2 \quad (9)$$

where

$$K_i(T) = -C_{1i}\cdot T\cdot\exp\left[-\frac{C_{2i}}{\left(T - T_g + 51.6\right)} - \frac{C_{3i}}{T\left(T_{mi} - T\right)^2}\right] \quad (10)$$

Here $K_i(T)$ are the crystallisation rate constants, T_{mi} are the crystal melt temperatures, n_i are the Avrami exponents, C_{1i}, C_{2i}, C_{3i} are the model constants, T_g is the glass transition temperature. Values of these constants are given in Ref. [23].

In this study, the annealing equation of Ref. [27] is modified to calculate the instantaneous value of crystallinity for a given instance, which can then be used as the initial value of crystallinity for the next time step. The normalised volume fraction of crystallinity for the i-th mechanism in the next time step $p + 1$, F_{vci}^{p+1} is found from the following expression:

$$\left[\ln\frac{1}{1 - F_{vci}^{p+1}}\right]^{1/n_i} = \left[\ln\frac{1}{1 - F_{vci}^{p}}\right]^{1/n_i} + \int_{t_p}^{t_{p+1}}\left[K_i(T(t))\right]^{1/n_i}\mathrm{d}t \qquad i = 1,2 \quad (11)$$

Therefore, the volume fraction of crystallinity at the next time step $p + 1$ can be obtained from:

$$c_v^{p+1} = c_v^{\infty}\left(w_1 F_{vc1}^{p+1} + w_2 F_{vc2}^{p+1}\right) \quad (12)$$

4. Residual stress model

A number of studies by several researchers were carried out to characterise development of residual thermal stresses during the post-manufacturing cool-down of composite laminates. Chapman et al. [1] developed a model to predict the macroscopic in-plane residual stresses induced in semi-crystalline thermoplastic composite laminates during cooling. They showed that the residual stress state was strongly influenced by the temperature gradients that occurred during processing, but weakly dependent on the level of crystallinity after processing. Eduljee et al. [28] developed a model to show the effect of crystallisation on the residual stress level. They found out that crystallisation resulted in an increase in residual stress levels through an increase in the resin modulus, and through modulus build-up at higher temperatures. On the other hand, the shrinkage due to crystallisation was found to have no effect on the residual stress development in neat PEEK, since the resin modulus at temperatures where the shrinkage occurs was very low. However, this model did not consider the effect of viscoelastic stress relaxation. Wang et al. [29] developed a numerical procedure to determine residual stresses and warpage for thermosets that could be applied to evaluate the effects of cool-down paths on the residual stresses and, thus, to optimise the curing cycle. The irreversible polymer shrinkage during curing was taken into consideration in this model. They also used a linear thermoviscoelastic lamination theory to analytically determine residual stresses and warpage in laminates. The numerical and analytical results came out to be in good agreement. Jeronimidis and Parkyn [30] determined the residual stresses in unbalanced cross-ply APC-2 laminates of various thicknesses manufactured with a cooling rate of 3°C/s by measuring the curvatures attained after processing. They also developed a model based on the CLT and measured thermoelastic properties of the APC-2 composite. They did not take into account the effect of crystallisation shrinkage. A 'stress free temperature' was defined as the temperature at which the curvature of the unbalanced cross-ply strips approached zero during heat up in the oven. This temperature was used in their model as the starting point of residual stress development. Kim et al. [31] studied the effect of cooling rate on residual stress development in a thermoplastic–matrix composite reinforced by graphite through monitoring warping of a cross-ply laminate. They showed that residual stresses in a cross-ply laminate were high enough to cause ply cracking. In another paper, Davies et al. [5] also examined the influence of cooling rate on short- and long-term properties of continuous fibre reinforced PEEK. They showed that slow cooling increased the degree of crystallinity of the matrix and reduced the level of internal stresses in multidirectional carbon fibre/PEEK laminates. On the other hand, unidirectional laminates showed little influence of cooling rate. Li et al. [32] developed a finite element residual stress model for thermoplastic composites. This model was based on a plane-strain elastic analysis with temperature-dependent matrix properties. The model was applied to $[0_{40}]_T$ unidirectional laminates to predict thermal residual stresses at surface cooling rates of 35°C/s and 10°C/s. Residual stress was found to decrease with reduced cooling rates. The same procedure was applied to $[0_{10}/90_6]_T$ non-symmetrical laminates with different surface cooling rates. This time the residual stresses increased as the cooling rate decreased. The results obtained showed that cooling rate differently affected these two types of laminates

due to the differences in the lay-up sequence and the crystallinity distribution. They stated that an appropriate processing cycle must be chosen for each specific lay-up in order to minimise the residual stresses and to optimise the mechanical performance of the composite laminates.

In this study, a 2D-plane-strain thermoviscoelastic finite element model was developed to predict residual stresses induced during cooling stage.

4.1. Formulation of the problem

4.1.1. Assumptions and constitutive relations

Although press moulding may accommodate fabrication of laminates having a curved shape with any preferred lay-up sequence, in this study a more basic geometry is chosen to simplify the analysis and interpret the results more easily. In our particular case, the plate is assumed to be flat with a unidirectional or a cross-ply lay-up. The width of the laminate is typically large enough to assume plane-strain state. Fig. 3 shows the laminate to be analysed and the coordinate system to be used.

The effect of crystallisation on residual stress development was assumed to be negligible as some previous studies [19,33] found it to be. It should also be noted that in order to incorporate crystallisation-shrinkage strain into the process-induced strain, a micromechanic model is needed, which predicts the behaviour of the composite from its constituents. As Barnes [34] indicated, reliability of these models is questionable. Therefore, consideration of this effect harbours an inherent risk of incurring a greater error.

In the analysis, linear constitutive relations are used. Displacement gradients $u_{i,j}$ are in absolute value much smaller than unity. Namely, the displacement changes slowly within the control volume. Material nonlinearity was also assumed to be negligible. In several studies [1,12,29,30,35], curvature of unbalanced APC-2 laminates was used as a measure of residual stresses induced during thermal processing. From these studies, it may be concluded that a significant portion of the residual stress builds up between just above the glass transition temperature (T_g) and the room temperature. Time dependent response of the material was reported to be dominated by the viscoelastic process close to T_g [36]. Nonlinear and viscoplastic effects can, therefore, be neglected without much compromising the accuracy of the results.

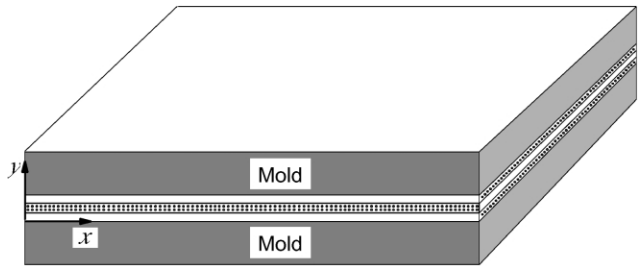

Fig. 3. The laminate in question and the coordinate system.

For a continuous unidirectional fibre-reinforced composite having a viscoelastic matrix, the creep compliances S_{11} and S_{12} can be taken to be independent of time and temperature [36,37], where '1' denotes the fibre direction and '2' denotes the transverse direction. Bearing in mind that the plane of the transverse isotropy is '2–3' plane, if the fibre direction of a ply coincides with the x direction, constitutive relations for the transversely isotropic viscoelastic ply are expressed as [38–40]

$$\epsilon_x(t) - \epsilon_x^*(t) = S_{11}\sigma_x(t) + S_{12}\sigma_y(t) + S_{12}\sigma_z(t)$$

$$\epsilon_y(t) - \epsilon_y^*(t) = S_{12}\sigma_x(t) + \int_0^t V_{22}(\tau)S_{22}(\xi - \xi')\frac{\partial\sigma_y(t)}{\partial\tau}\mathrm{d}\tau + \int_0^t V_{23}(\tau)S_{23}(\xi - \xi')\frac{\partial\sigma_z(t)}{\partial\tau}\mathrm{d}\tau$$

$$2\epsilon_{xy}(t) = \int_0^t V_{66}(\tau)S_{66}(\xi - \xi')\frac{\partial\sigma_{xy}(t)}{\partial\tau}\mathrm{d}\tau \tag{13}$$

where $\epsilon_x^*(t)$ and $\epsilon_y^*(t)$ are the thermal strains. Since the thermal expansion coefficients are temperature dependent, they are given by

$$\epsilon_i^*(t) = \int_{T_0}^{T_f} \alpha_i(T)\mathrm{d}T \tag{14}$$

ξ is the pseudo time, which explains the dependence of the creep compliance on temperature. It is given by

$$\xi = \int_0^t a[T(\eta)]d\eta \text{ and } \xi' = \int_0^\tau a[T(\eta)]d\eta \tag{15}$$

$a(T)$ is the shift factor, which is related to the amount of horizontal shift required to make the modulus–time curve for temperature T coincide with the one corresponding to the base temperature T_{base}. When T is less than T_{base}, then $a(T)$ takes a value smaller than 1. When T is greater than T_{base}, $a(T)$ takes a value greater than 1. This means that accelerated viscoelastic processes within the material due to increased temperature are reflected in a faster elapse of time. $V(T)$ is the vertical shift factor introduced to account for the decrease in the value of the long-term creep compliance $S(\infty)$ with an increase in temperature.

When the fibre direction of a ply, '1', is transverse to the $x$direction, the constitutive relations become

$$\epsilon_x(t) - \epsilon_x^*(t) = \int_0^t V_{22}(\tau)S_{22}(\xi - \xi')\frac{\partial\sigma_x(\tau)}{\partial\tau}\mathrm{d}\tau + \int_0^t V_{23}(\tau)S_{23}(\xi - \xi')\frac{\partial\sigma_y(\tau)}{\partial\tau}\mathrm{d}\tau + S_{12}\sigma_z(t)$$

$$\epsilon_y(t) - \epsilon_y^*(t) = \int_0^t V_{23}(\tau)S_{23}(\xi - \xi')\frac{\partial\sigma_x(\tau)}{\partial\tau}\mathrm{d}\tau + \int_0^t V_{22}(\tau)S_{22}(\xi - \xi')\frac{\partial\sigma_y(\tau)}{\partial\tau}\mathrm{d}\tau + S_{12}\sigma_z(t)$$

$$2\epsilon_{xy}(t) = \int_0^t [S_{22}(\xi - \xi') - S_{23}(t - \tau)]\frac{\partial\sigma_{xy}(\tau)}{\partial\tau}\mathrm{d}\tau \tag{16}$$

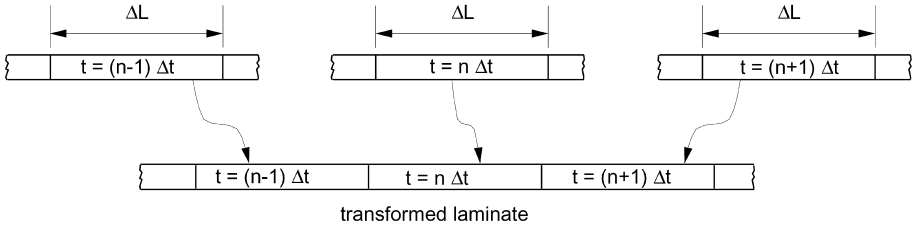

Fig. 4. Transformed solution domain.

The usual procedure of determining the final residual stress levels is to calculate the stresses at different time steps of the cooling process through a viscoelastic analysis and add the incremental stresses obtained in each step. However, this procedure results in excessive computational times for the optimisation process, in which convergence to minimum requires hundreds of residual stress computations. Instead, we follow a different approach. First, we assume the plate to be so large that edge effects are negligible. Accordingly, our problem is the determination of residual stresses in an symmetric infinite laminate where the temperature is varying only in the thickness direction. Let us consider a strip of the laminate with length ΔL at discrete times ($t = 0$, Δt, $2\Delta t$, …, $(n-1)\Delta t$, $n\Delta t$, $(n+1)\Delta t$, …, t_f). Then, we compose a new laminate by joining together the strips as shown in Fig. 4. The larger value we choose for ΔL and the smaller for Δt, the closer will be the values of the stresses obtained through the viscoelastic analysis of the transformed laminate to the exact value. The stress state of the laminate at a given time t' is then taken to be equivalent to the stress state of the transformed laminate at the location of $x = t'\Delta L/\Delta t$. Since at the end of cooling there will be no change in stress levels with time, the stress state at the right hand of the transformed laminate represents the residual stresses.

4.1.2. Boundary conditions

In the press moulding process of thermoplastic composites, when the temperature is above the glass transition point, pressure should be applied in order to suppress void formation within the matrix. Since we neglect material nonlinearity, which means material properties are independent of stress level, an external pressure does not alter the values of residual stresses in our stress analysis. Therefore, mould pressure is not included as a boundary condition. Only vertical displacement was set to zero at the centre due to the symmetry of the laminate.

$$u_y = 0 \text{ at the centre, } y = h/2 \tag{17}$$

Because at the beginning of cooling the matrix is in the melt state, stresses may not develop. Therefore, stresses at the left end of the transformed solution domain are zero:

$$\sigma_{xx} = 0 \tag{18}$$

4.2. Finite element solution of the problem

The transformed laminate to be analysed is divided into eight-degrees-of-freedom rectangular elements as shown in Fig. 5. The temperature of a node i in the transformed domain is taken as the temperature of the laminate at position y_i and at time $t = x_i/(\Delta L/\Delta t)$, where x_i is the abscissa of the node in the transformed domain.

The strain in a finite element is a linear function of the eight nodal displacements [41] as in the elastic analysis:

$$\{\epsilon\}_r = [A]_r\{\delta\}_r \tag{19}$$

where $[A]_r$ is a 3×8 matrix whose elements depend only on the nodal displacements of the element r, $\{\delta\}_r$.

The viscoelastic memory of the material is reflected by the stress state in a given element being influenced by the strains in all the elements through which the material previously passed [42,43]. Considering the quasi-steady state assumption, in which stress and strain states in the control volume do not change with time, the strain history of a material occupying a particular element can be estimated from the current configuration. For example, the material occupying the element n (Fig. 5) was in the elements 1, 2, 3, …, $n-1$ at times, t_1, t_2, t_3, …, t_{n-1} and had the same stress and strain state as the materials occupying these elements at the present time. Thus, the stress components in the finite element n (Fig. 5) are found by adding the contributions by all the elements through which the material has previously passed. This can be done by converting the convolution integrals in Eq. (13) (or Eq. (16)) into a summation of series and reducing the

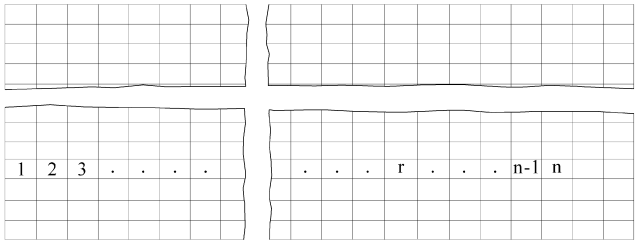

Fig. 5. Mesh structure used in the stress analysis. Horizontal and vertical dimensions are not on scale.

relation to the following form (Appendix A):

$$\begin{Bmatrix} \sigma_x^n \\ \sigma_y^n \\ \sigma_{xy}^n \end{Bmatrix} = \sum_{r=1}^{n} \begin{bmatrix} c_{11}^{nr} & c_{12}^{nr} & 0 \\ c_{12}^{nr} & c_{22}^{nr} & 0 \\ 0 & 0 & c_{66}^{nr} \end{bmatrix} \begin{Bmatrix} \epsilon_x^r - \epsilon_x^{*r} \\ \epsilon_y^r - \epsilon_y^{*r} \\ 2\epsilon_{xy}^r \end{Bmatrix} \tag{20}$$

or more concisely

$$\{\sigma\}_n = \sum_{r=1}^{n} [C]_{nr}\{\epsilon\}_r - \sum_{r=1}^{n} [C]_{nr}\{\epsilon^*\}_r \tag{21}$$

where $\{\epsilon^*\}$ is the thermal strain vector [44] whose elements depend only on the nodal temperatures of the element r. Combining Eqs. (19) and (21), we obtain

$$\{\sigma\}_n = \sum_{r=1}^{n} [C]_{nr}[A]\{\delta\}_r - \sum_{r=1}^{n} [C]_{nr}\{\epsilon^*\}_r \tag{22}$$

The virtual work principle is written as

$$\{\delta\}_n^T\{F\}_n = \int_V \{\epsilon\}_n^T\{\delta\}_n \mathrm{d}V \tag{23}$$

where $\{F\}_n$ is the vector of forces acting at the nodal points of the element n, and V is its volume. Substituting Eqs. (19) and (22) into Eq. (23), we have

$$\{\delta\}_n^T\{F\}_n = \int_V \{\delta\}_n^T\{A\}_n^T \left[\sum_{r=1}^{n} [C]_{nr}[A]_r\{\delta\}_r - \sum_{r=1}^{n} [C]_{nr}\{\epsilon^*\}_r \right] \mathrm{d}V \tag{24}$$

By equating the terms in front of the nodal displacement vector $\{\delta\}$, we obtain

$$\{F\}_n = \int_V \sum_{r=1}^{n} [A]_n^T[C]_{nr}[A]_r\{\delta\}_r \mathrm{d}V - \int_V \sum_{r=1}^{n} [A]_n^T \times [C]_{nr}\{\epsilon^*\}_r \mathrm{d}V \tag{25}$$

or,

$$\{F\}_n = \sum_{r=1}^{n} [K]_{nr}\{\delta\}_r + \sum_{r=1}^{n} \{H\}_{nr} \tag{26}$$

Here $[K]_{nr}$ is the effective element stiffness matrix given by

$$[K]_{nr} = \int_V [A]_n^T[C]_{nr}[A]_r \mathrm{d}V \tag{27}$$

$\{H\}_{nr}$ is the effective thermal force vector.

$$\{H\}_{nr} = -\int_V [A]_n^T[C]_{nr}\{\epsilon^*\}_r \mathrm{d}V \tag{28}$$

Components of the element stiffness matrix and the thermal force vector are given in Ref. [45]. Assembling all the element stiffness matrices and the thermal force vectors for the entire control volume, we obtain

$$\{F\} = [K]\{\delta\} + \{H\} \tag{29}$$

where $[K]$ is the $2m \times 2m$ global stiffness matrix, m being the number of nodes, $\{F\}$ is the force vector, $\{\delta\}$ is the displacement vector, and $\{H\}$ is the thermal force vector. The factor 2 indicates the two degrees of freedom at each node. The global stiffness matrix $[K]$ is unsymmetric and banded.

Eq. (29) is the equilibrium equation to be solved together with the boundary conditions. First, Eq. (29) is rearranged as

$$\begin{Bmatrix} F_f \\ F_r \end{Bmatrix} = \begin{bmatrix} K_{ff} & K_{fr} \\ K_{rf} & K_{rr} \end{bmatrix} \begin{Bmatrix} \delta_f \\ \delta_r \end{Bmatrix} + \begin{Bmatrix} H_f \\ H_r \end{Bmatrix} \tag{30}$$

where the subscript r represents the restrained degrees of freedom, while f denotes the free ones. Since

$$\{\delta_r\} = \{0\} \tag{31}$$

the final system of equations to be solved becomes

$$\left\{F_f\right\} = \left[K_{ff}\right]\left\{\delta_f\right\} + \left\{H_f\right\} \tag{32}$$

After determining the unknown nodal displacements $\{\delta_f\}$, strains in each finite element are obtained by using Eq. (19). From Eq. (22), the stress field within the control volume is determined. Residual stresses are the stresses at the right end of the control volume, which corresponds to the stress state at the end of cooling.

5. Optimisation

The optimisation methods may be classified as zero order methods, that need only evaluations of the objective and constraint functions and high order methods that also require derivative evaluations of these functions. It should be noted that we adopted a numerical approach and consequently cannot predict temperature profiles and residual stresses in closed form. In order to avoid the difficulty of obtaining their numerical derivatives, we preferred a zero order method called the sequential simplex (Nelder–Mead) method [46]. In addition, in order to handle the constraint violations, penalty functions were used. The constrained optimisation problem was, thus, transformed into an unconstrained one for which the algorithm was suitable.

In order for the optimisation algorithm to generate a new cooling curve in every iteration, the cooling curves need to be described by a finite number of design variables so that by altering these variables, a new cooling curve can be obtained. Furthermore, for a press moulding equipment to deliver the specified cooling scheme its time derivatives should be continuous, i.e. the curve should be smooth. In this respect, it is suitable to describe a cooling scheme by spline curves passing through keypoints that serve as design variables. A typical cooling curve described by keypoints is shown in Fig. 6. Time interval between any two adjacent keypoints, Δt_{kp}, is the same. Keypoints formed by T_k ($k = 1, 2, \ldots, N-1$) and Δt_{kp} make up a set of N design variables. Since the consolidation temperature, T_c ($= T_0$), and the final

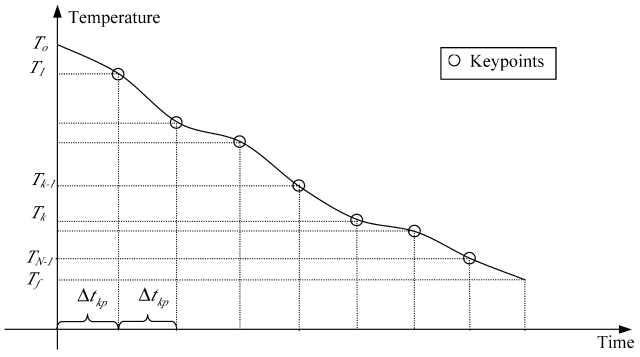

Fig. 6. A typical cooling curve for the surface of the laminate.

temperature, T_f ($= T_N$), at which the laminate is taken out from the mould, are known, they are taken to be constants. By repositioning these keypoints, i.e. assigning a different temperature, T_k, or time interval, Δt_{kp}, and fitting spline curves through these keypoints, a different and at the same time smooth cooling curve for the surface of the laminate is obtained. This will constitute the boundary condition for the heat transfer analysis that is to be carried out to find the temperature distribution within the laminate.

5.1. The quality constraints

A thermoplastic composite basically should satisfy four quality criteria in order to exhibit the desired performance. Firstly, it should be fully consolidated; i.e. void free. Secondly, thermal degradation should be avoided. Thirdly, residual stresses should not be excessive and, lastly, crystallinity should be within the recommended range. Since the composite is to be kept in the molten state sufficiently long, we may assume that the first criterion is already satisfied before the onset of cooling. It can also be assumed that the moulding time is short enough not to cause any thermal degradation. For example, maximum processing time for APC-2 thermoplastic composites at 400°C is 2 h [47], while the moulding time is 25 min [48]. On the other hand, satisfaction of the other two criteria depends on the cooling scheme and, therefore, imposes constraints on the optimisation process.

5.1.1. The constraint on maximum residual stress

Maximum residual stress, σ_R, should be less than the maximum allowable stress, σ_R^{all}. Accordingly, the constraint equation is

$$\sigma_R < \sigma_R^{all} \tag{33}$$

For APC-2, σ_R^{all} was chosen based on the standard cooling rate (0.25°C/s) recommended by ICI [48]. Using the residual stress analysis, maximum allowable residual stress corresponding to the standard cooling scheme was determined as 74 MPa.

5.1.2. The constraint on crystallinity

Crystallinity of a semi-crystalline polymer is known to affect its mechanical properties. In order to avoid post-processing, the crystallinity of the final product should be within the recommended levels. Then,

$$c_m^{min} < c_m < c_m^{max} \tag{34}$$

where c_m is the mass fraction of crystallinity As for APC-2, recommended levels of crystallinity are between 25 and 35% [47].

5.2. Constraints regarding the cooling curve

If our cooling scheme is not to contain annealing, temperatures of the keypoints should be in decreasing order. This means

$$T_k < T_{k-1} \qquad k = 1, \ldots N \tag{35}$$

It should be noted that although the temperatures of the keypoints are decreasing, $T(t)$ is not necessarily so. Spline curves may allow occasional increases in the curve.

Since press-moulding equipment may not deliver very high cooling rates, sudden temperature drops should be avoided. The constraint equation may then be expressed as

$$\frac{T(t_n, 0) - T(t_{n+1}, 0)}{\Delta t} \leq CR_{max} \qquad n = 0, 1, \ldots \tag{36}$$

where $T(t_n, 0)$ and $T(t_{n+1}, 0)$ are the values of temperature at the surface of the laminate ($y = 0$) for the n-th and $(n + 1)$-th time steps, respectively. Maximum cooling rate (CR_{max}) depends on the capacity of the press moulding equipment.

Another constraint was used to prevent the value of Δt_{kp} from getting negative values during the optimisation process. So, the constraint equation is

$$\delta t_{kp} > 0 \tag{37}$$

5.3. Objective function

The objective function to be minimised is actually the cooling time. However, violations of the constraints in Eqs. (33)– (36) are expressed as penalty functions to constitute part of the objective function. By penalising any excursion into the infeasible region, the algorithm is forced to search the minimum within the feasible region and thus convergence into a minimum point within the infeasible region is avoided. The objective function is constructed as

$$f = t_c(1 + P_1 + P_2 + P_3 + P_4 + P_5) \tag{38}$$

where P_i are the penalty functions corresponding to the aforementioned constraints and t_c is the cooling time given by

$$t_c = N\Delta t_{kp} \tag{39}$$

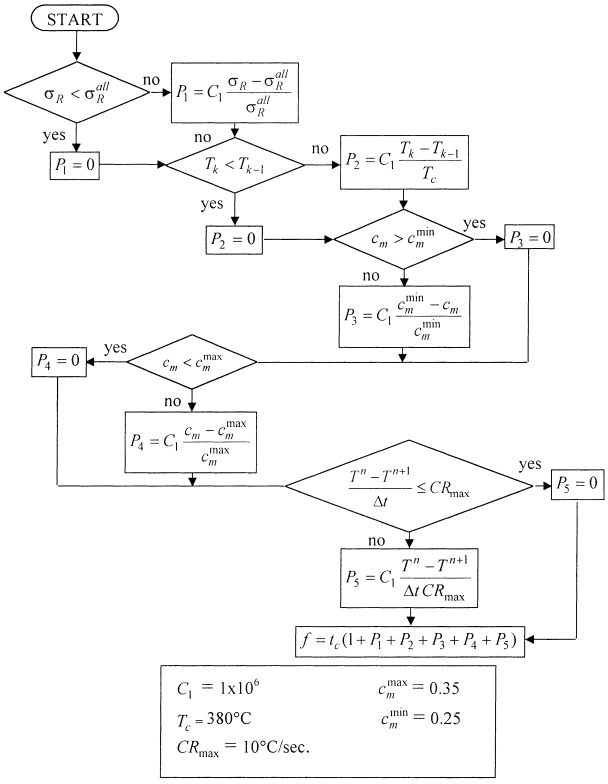

Fig. 7. The procedure for the calculation of the objective function.

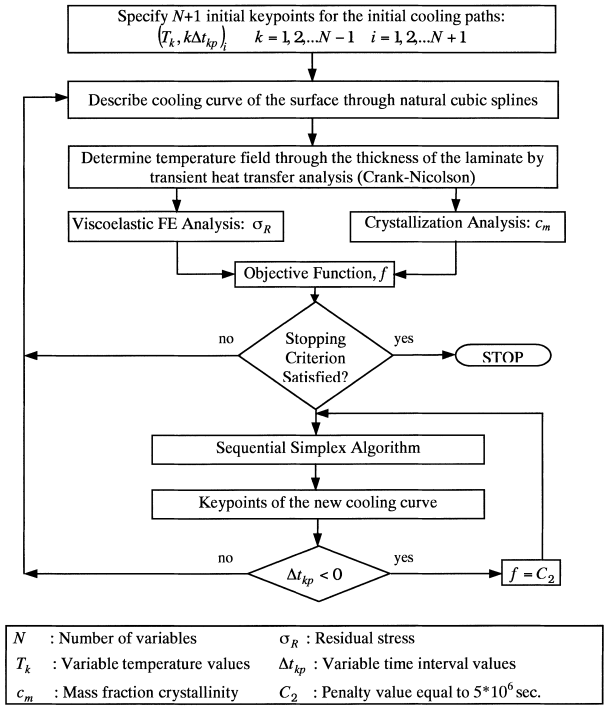

Fig. 8. A flowchart presentation of the cooling time minimisation scheme.

where N is the number of time intervals. The procedure to calculate the objective function is described in Fig. 7.

5.4. Optimisation procedure

The goal of the optimisation procedure is to find the set of design variables that will result in the minimum cooling time in press moulding while satisfying all the aforementioned constraints. The design variables are the temperatures at the keypoints and the time interval between them. A flowchart of the optimisation procedure is presented in Fig. 8.

The optimisation algorithm, sequential simplex, requires $N + 1$ initial sets of these variables to construct $N + 1$ cooling paths. After specifying $N + 1$ sets of keypoints randomly, cooling paths are formed by spline curves passing through the keypoints. Corresponding to each cooling path, temperature profiles through the thickness of the laminate are obtained by using the transient heat transfer model. Next, maximum residual stress and mass fraction crystallinity values for these initial cooling schemes are determined by plain-strain-viscoelastic-finite element and crystallisation kinetics analyses, respectively. Then, an objective function, f, is calculated for each cooling path, as explained in Section 5.3. and Fig. 7. All these steps provide us with the information needed to initiate the sequential simplex algorithm. The algorithm replaces the worst of these sets at every iteration by another set having a better objective function value. These steps are repeated until the following stopping criterion is met:

$$\left\{ \frac{1}{N+1} \sum_{i=1}^{N} [f_i - \bar{f}]^2 \right\}^{1/2} < \epsilon \tag{40}$$

$$\bar{f} = \frac{1}{N+1} \left(\sum_{i=1}^{N} f_i \right) \tag{41}$$

where N is the number of variables, ϵ is a sufficiently small number, i.e. the tolerance, and $\bar{f}$ is the average of objective function values of $N + 1$ cooling paths for the current iteration. In case the simplex algorithm produces a negative value for the time interval between the keypoints, a penalty value, C_2, is assigned to the objective function without constructing the cooling path and carrying out the analyses.

In order to guarantee convergence to the global minimum, optimisation process should be repeated many times, starting from different points within the design space. Then, the cooling path having the minimum objective function value is chosen as the global optimum path.

Table 1
Vertical shift factors for APC-2

Temperature (°C)	Vertical shift factor (log V)
40	− 0.025
129.4	+ 0.0031
200	+ 0.21

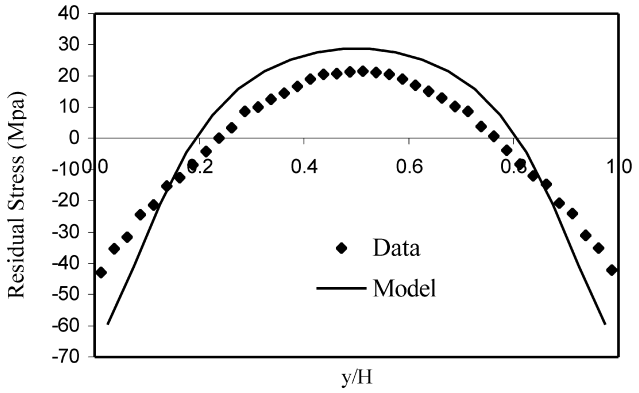

Fig. 9. Transverse normal residual stress distribution within a 40 ply APC-2 unidirectional laminate, $[0_{40}]_T$, processed by press moulding at a 35°C/s surface cooling rate. Experimental data were obtained by a layer removal technique [53].

6. Results and discussions

6.1. Inputs

Computer codes were developed to determine temperature and residual stress distributions following the aforementioned solution procedure. The processed material was chosen to be APC-2, which has prepreg thickness of 0.125 mm [47]. The data provided by Grove [49] were used for the thermal conductivity and specific heat. Density of the material for a range of temperatures was measured by Blundell and Willmouth [50].

Most of the inputs for APC-2 used in the stress analysis were given in Ref. [44]. Xiao [36] provided the data regarding the creep compliances and the shift factors. Vertical shift factors reported by Xiao [36] were extrapolated as done in Refs. [17,51] (Table 1).

Barnes [34,52] characterised the anisotropic thermal expansion behaviour of APC-2. Jeronimidis and Parkyn [30] determined the stress free temperature by heating up

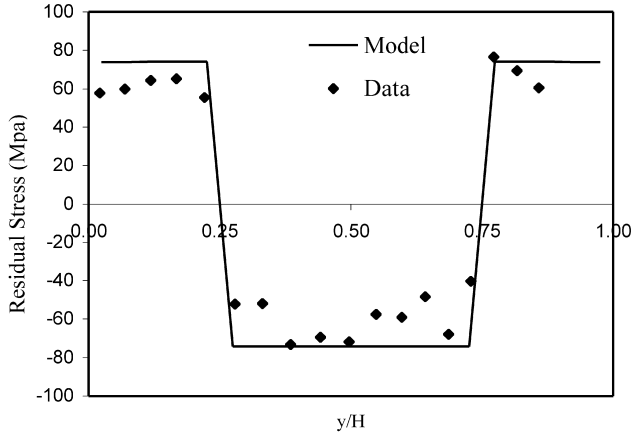

Fig. 10. Normal stress distribution within a cross-ply laminate, $[0_{10}/90_{10}]_S$, processes by press moulding at a 0.25°C/s surface cooling rate. Experimental data were obtained by a layer removal technique [54].

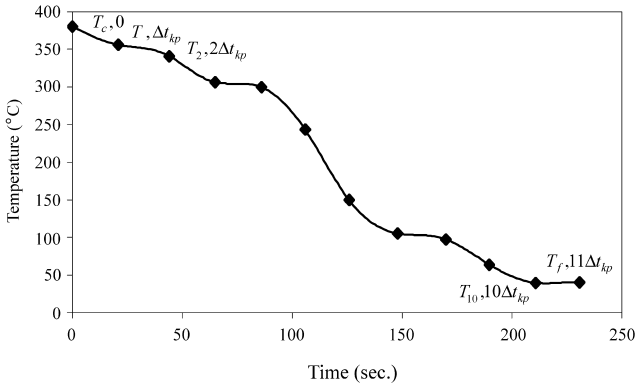

Fig. 11. Optimal cooling curve for APC-2 $[90_{10}/0_{10}]_S$ laminate for $CR_{max} = 5$°C/s.

unbalanced laminates and observing the temperature at which they became flat. They found it to be 310°C. In another study [12], the stress free temperature was found to be 280°C. However, the residual stress model was observed to be not very sensitive to the value of stress free temperature. The results did not show appreciable difference for the two values of stress free temperature. In this study, base temperature, T_{base}, was taken to be 280°C and the effect of thermal expansion on residual stress development was neglected above this temperature by taking thermal expansion coefficients as zero.

After an extensive convergence test on the residual stress model, 86×20 mesh, totalling 1827 nodes, was observed to yield accurate results, and the length of the transformed solution domain was set to 1.4 m. $\Delta L/\Delta t$ is then equal to the ratio of this length to the total time, which is longer than the cooling time. Times that elapse before the onset of cooling and after the end of cooling are also accounted for in the transformed domain to minimise the edge effects.

6.2. Verification

In order to verify our models, the numerical results were compared with experimental results for two different cases.

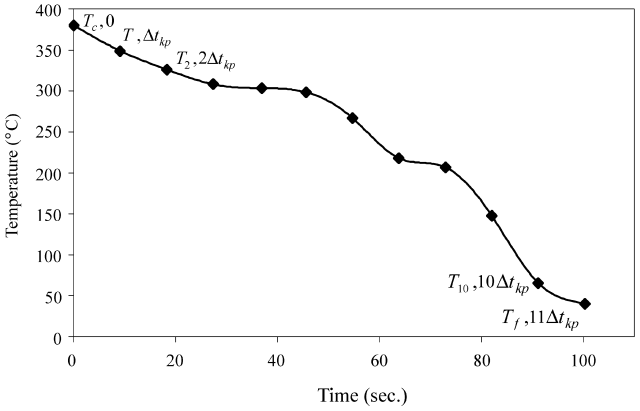

Fig. 12. Optimal cooling curve for APC-2 $[90_{10}/0_{10}]_S$ laminate for $CR_{max} = 10$°C/s.

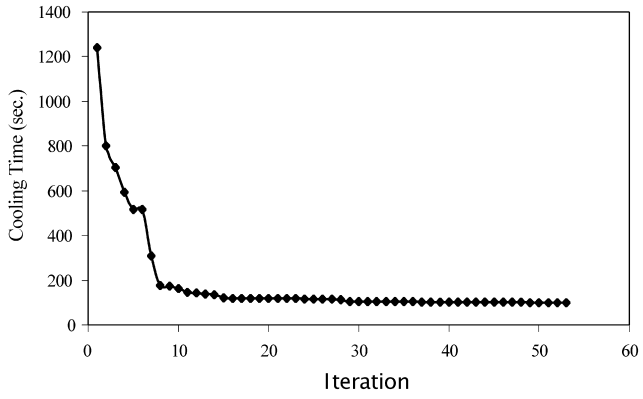

Fig. 13. Variation of the cooling time during optimisation for $CR_{max} = 10°C/s$.

One is for a unidirectional laminate, $[0_{40}]$, processed at 35°C/s surface cooling rate, the other is for a cross-ply laminate, $[0_{10}/90_{10}]_S$ processed at 0.25°C/s surface cooling rate. As seen in Figs. 9 and 10, predictions of the residual stress model agree quite well with the experimental data, although the model slightly overestimates. This may be due to nonlinear viscoelastic effects, which are neglected in the model, or due to some transverse cracks developed in the specimen during processing which locally relieve residual stresses.

6.3. Optimum cooling curves

The aforementioned optimisation procedure was used to obtain the optimum process parameters that lead to the minimisation of cooling time for APC-2 $[0_{10}/90_{10}]_S$ laminates. The resulting optimal cooling curves for two different maximum cooling rates are illustrated in Figs. 11 and 12. The markers on the curves represent the keypoints through which the natural cubic spline curve is plotted. The initial and final temperatures T_0 and T_f on the curve are 380 and 40°C, respectively. 380°C is the consolidation temperature recommended by ICI for APC-2 [48]. The surface temperature at which the laminate can safely be taken out from the mould was considered to be 40°C. Cooling process is, therefore, terminated at this temperature. Inner temperature, on the other hand, was observed to be 127°C for the fastest cooled laminate. Considering that this is below the glass transition temperature, delaminations or void formation due to removal of pressure are not expected.

Total cooling times, t_c, for the two cases were 100.3 and 230.7 s. They are quite low compared to the cooling time in the standard scheme [48], which is about 25 min. Further decrease in cooling time was not possible, because higher cooling rates resulted in either high residual stresses or crystallinity levels that are not recommended.

The variation of the cooling time during the optimisation process for a cooling rate of 10°C/s is given in Fig. 13. The infeasible design points where the penalty function was employed are not included in this figure. The total number of iterations was 344. Total CPU time was about 15 h for Pentium III.

6.4. Residual stress distribution

Fig. 14 illustrates the final distribution of residual stresses through the thickness of the APC-2 $[90_{10}/0_{10}]_S$ laminate corresponding to the optimal cooling curve for two different cooling rates. The distribution is symmetric as expected. Residual stresses at the top and bottom ten 90° plies are tensile whereas they are compressive for the middle 20 plies oriented in 0° direction. Maximum residual stress is less than the residual stress developed during standard cooling. For example, for a maximum cooling rate of 10°C/s, the maximum residual stress value is 73.69 MPa and it occurs twice at *y*/*h* values of 0.225 and 0.775. These points correspond to the ninth and 31st plies, respectively.

6.5. Crystallinity

Fig. 15 illustrates development of crystallinity at the surface of the APC-2 $[90_{10}/0_{10}]_S$ laminate for the corresponding optimal cooling curve. As seen from the figure, crystallinity approaches to the minimum allowed mass fraction crystallinity, 0.25 in both cases.

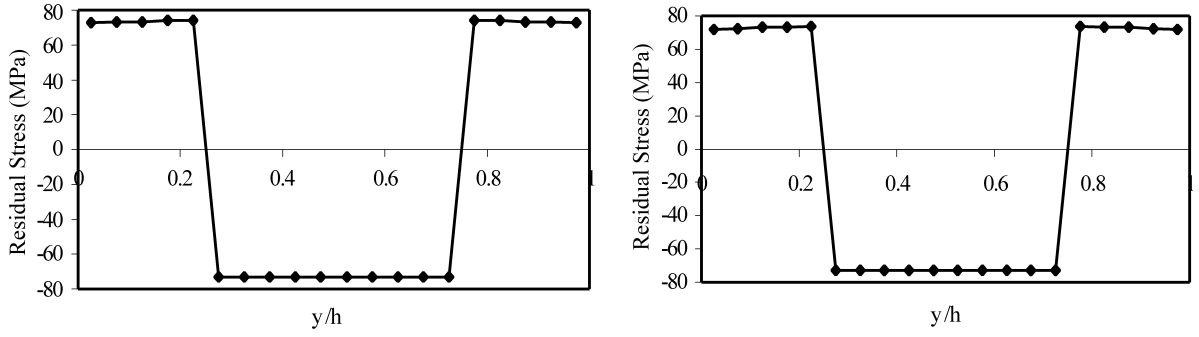

Fig. 14. Final residual stress distributions corresponding to the optimal cooling curve for $CR_{max} = 5$ and 10°C/s, respectively.

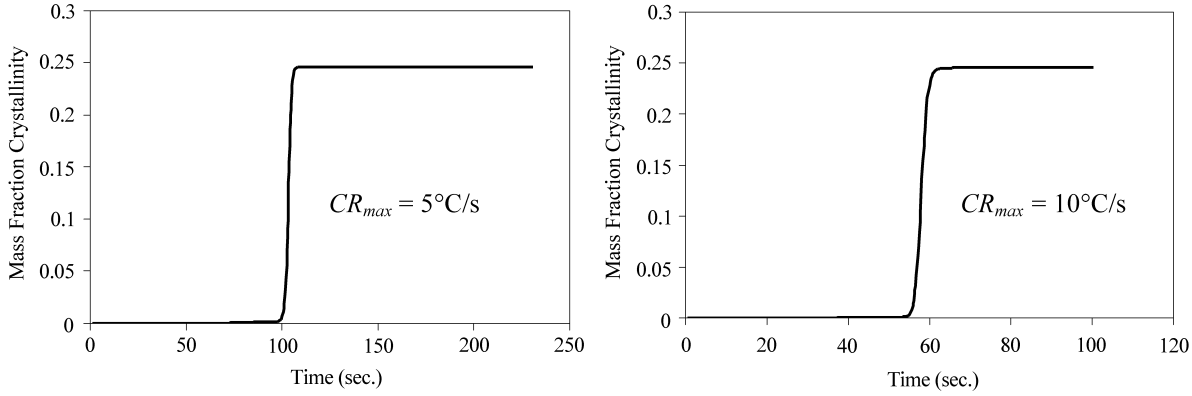

Fig. 15. Mass fraction crystallinity values corresponding to the optimal cooling curve for $CR_{max} = 5$ and 10°C/s.

7. Conclusions

In the present study, optimisation of the cooling stage of the press moulding process was carried out in order to minimise the cooling time. Heat transfer, crystallisation and residual stress models were integrated into an optimisation algorithm to accomplish this task. The optimisation algorithm, called sequential simplex, was employed in order to determine the cooling paths that result in the minimum cooling time with desired quality of the moulded part. It was noticed that the quality constraints, i.e. crystallisation and residual stress, were very influential on the final results. We achieved significant reduction in the cooling time without compromising the quality in comparison to the standard cooling scheme for APC-2. Results were obtained for two different values of maximum cooling rates. The minimum cooling times were 100.3 and 230.7 s for maximum cooling rates of 10 and 5°C/s, respectively, as opposed to the 25 min of standard cooling time. Since, with larger number of keypoints, the number of possible configurations for cooling paths within which the algorithm searches the minimum increases, better results can be obtained. However, the computational burden also increases due to the increased number of design variables. Our choice of 10 keypoints seems to be a good compromise.

The optimisation procedure developed in this study can be adapted to residual stress minimisation problem by modifying the objective function accordingly.

Acknowledgements

This paper is based on the work supported by the Research Fund of Bogazici University with the code number 99A603.

Appendix A. Numerical integration of the constitutive equations

Rewriting constitutive equation for shear strain given in Eq. (13), we have

$$2\epsilon_{xy}(t) = \int_0^t V_{66}(T(\tau))S_{66}(\xi(t) - \xi'(t))\frac{\partial\sigma_{xy}(\tau)}{\partial\tau}\mathrm{d}\tau \qquad (A.1)$$

where *pseudo-time*, ξ, is related to the real time by

$$\xi = \int_0^t a[T(x_i, \eta)]\mathrm{d}\eta \qquad (A.2)$$

where $a(T)$ is the *horizontal shift factor*. The above integral can easily be calculated numerically. Applying integration by parts to Eq. (A.1), one obtains

$$2\epsilon_{xy}(t) = \sigma_{xy}(\tau)V_{66}(T(\tau))S_{66}(\xi(t) - \xi'(t))\big|_0^t - \int_0^t \sigma_{xy}(\tau)\frac{\partial[V_{66}(T(\tau))S_{66}(\xi(t) - \xi'(t))]}{\partial\tau}\mathrm{d}\tau \qquad (A.3)$$

then,

$$2\epsilon_{xy}(t) = \sigma_{xy}(t)V_{66}(T(\tau))S_{66}(0) - \sigma_{xy}(0)V(T(0))S_{66}(\xi(t)) - \int_0^t \sigma_{xy}(\tau)\frac{\partial[V_{66}(T(\tau))S_{66}(\xi(t) - \xi'(t))]}{\partial\tau}\mathrm{d}\tau \qquad (A.4)$$

where the second term explains the initial stress. Since stresses are zero at the beginning of cooling, this term does not contribute to strains.

Eq. (A.4) can be integrated by finite differences in time increments t_i or $\xi_i(t_i)$ $(i = 1, 2, \ldots r, \ldots n)$, where t_r is the time at which the material was in finite element r (Fig. 5), ($t_1 = 0$ and $t_n = t$). Then, by utilising the second mean value theorem, one obtains the strain in finite element n:

$$2\epsilon_{xy} = (t_n)V_{66}(T_n)S_{66}(0) - \frac{1}{2}\sum_{r=1}^{n-1}\left[\sigma_{xy}(t_{r+1}) + \sigma_{xy}(t_r)\right] \times [V_{66}(T_{r+1})S_{66}(\xi_n - \xi_{r+1}) - V_{66}(T_r)S_{66}(\xi_n - \xi_r)] \qquad (A.5)$$

By following the above procedure for ϵ_y Eq. (13) can be

reduced to the following form:

$$\begin{Bmatrix} \epsilon_x(t_n) \\ \epsilon_y(t_n) \\ 2\epsilon_{xy}(t_n) \end{Bmatrix} = \sum_{r=1}^{n} \begin{bmatrix} d_{11}^{nr} & d_{12}^{nr} & 0 \\ d_{12}^{nr} & d_{22}^{nr} & 0 \\ 0 & 0 & d_{66}^{nr} \end{bmatrix} \begin{Bmatrix} \sigma_x(t_r) \\ \sigma_y(t_r) \\ \sigma_{xy}(t_r) \end{Bmatrix} + \begin{Bmatrix} \epsilon_x^*(t_n) \\ \epsilon_y^*(t_n) \\ 0 \end{Bmatrix} \tag{A.6}$$

or

$$\{\epsilon\}_n = \sum_{r=1}^{n} [D]_{nr}\{\sigma\}_r + \{\epsilon^*\}_n$$

where

$$d_{11}^{nr} = \begin{cases} 0 & r \neq n \\ S_{11} & r = n \end{cases} \tag{A.7}$$

$$d_{12}^{nr} = \begin{cases} 0 & r \neq n \\ S_{12} & r = n \end{cases} \tag{A.8}$$

$$d_{22}^{nr} = \begin{cases} -\frac{1}{2}\{V_{22}(T_1)S_{22}(\xi_n) + V_{22}(T_2)S_{22}(\xi_n - \xi_2)\} & r = 1, n \neq 1 \\ \frac{1}{2}\{V_{22}(T_{r-1})S_{22}(\xi_n - \xi_{r-1}) - V_{22}(T_{r+1})S_{22}(\xi_n - \xi_{r+1})\} & 1 < r < n \\ V_{22}(T_1)S_{22}(\xi_1) & r = n = 1 \\ \frac{1}{2}\{V_{22}(T_{n-1})S_{22}(\xi_1) + V_{22}(T_n)S_{22}(\xi_n - \xi_{n-1})\} & r = n \neq 1 \end{cases} \tag{A.9}$$

$$d_{66}^{nr} = \begin{cases} -\frac{1}{2}\{V_{66}(T_1)S_{66}(\xi_n) + V_{66}(T_2)S_{66}(\xi_n - \xi_2)\} & r = 1, n \neq 1 \\ \frac{1}{2}\{V_{66}(T_{r-1})S_{66}(\xi_n - \xi_{r-1}) - V_{66}(T_{r+1})S_{66}(\xi_n - \xi_{r+1})\} & 1 < r < n \\ V_{66}(T_1)S_{66}(\xi_1) & r = n = 1 \\ \frac{1}{2}\{V_{66}(T_{n-1})s_{66}(\xi_1) + V_{66}(T_n)S_{66}(\xi_n - \xi_{n-1})\} & r = n \neq 1 \end{cases} \tag{A.10}$$

Strain–stress relations given by Eq. (A.6)) in numerical form are valid for plane stress. However, in our model, we assumed plane-strain state. For plane strain, when the x direction and the fibre direction, '1', coincide, (Eq. (A.6)) becomes

$$\begin{Bmatrix} \epsilon_x(t) \\ \epsilon_y(t) \\ 2\epsilon_{xy}(t) \end{Bmatrix} = \sum_{r=1}^{n} \begin{bmatrix} d_{11}^{nr} - (d_{12}^{nr})^2/d_{22}^{nr} & d_{12}^{nr} - d_{12}^{nr}d_{23}^{nr}/d_{22}^{nr} & 0 \\ d_{12}^{nr} - d_{12}^{nr}d_{23}^{nr}/d_{22}^{nr} & d_{22}^{nr} - (d_{23}^{nr})^2/d_{22}^{nr} & 0 \\ 0 & 0 & d_{66}^{nr} \end{bmatrix} \times \begin{Bmatrix} \sigma_x(t_r) \\ \sigma_y(t_r) \\ \sigma_{xy}(t_r) \end{Bmatrix} + \begin{Bmatrix} \epsilon_x^*(t) \\ \epsilon_y^*(t) \\ 0 \end{Bmatrix} \tag{A.11}$$

where, d_{23}^{nr} is the same as d_{22}^{nr} in Eq. (A.9) except that S_{23} is used instead of S_{22}. Assuming that Poisson's ratio in the isotropic plane ν_{23} is independent of time and temperature, $S_{23}(t)$ is given by

$$S_{23}(t) = -\nu_{23}S_{22}(t) \tag{A.12}$$

Also, in plane strain state, the following values should be used for thermal expansion coefficients:

$$\alpha_{xx} = \alpha_{11} + \nu_{31}\alpha_{33} \qquad \alpha_{yy} = \alpha_{22} + \nu_{32}\alpha_{33} \tag{A.13}$$

where, '1' shows the fibre direction and '2' and '3' show the transverse directions. For transversely isotropic laminates $\alpha_{33} = \alpha_{22}$, $\nu_{32} = \nu_{23}$ and $\nu_{31} = \nu_{21}$.

When the x direction is transverse to the fibre direction for a given ply, strain–stress relations for plane strain become

$$\begin{Bmatrix} \epsilon_x(t) \\ \epsilon_y(t) \\ 2\epsilon_{xy}(t) \end{Bmatrix} = \sum_{r=1}^{n} \begin{bmatrix} d_{22}^{nr} - (d_{12}^{nr})^2/d_{11}^{nr} & -\nu_{23}d_{22}^{nr} - (d_{12}^{nr})/d_{11}^{nr} & 0 \\ -\nu_{23}d_{22}^{nr} - (d_{12}^{nr})/d_{11}^{nr} & d_{22}^{nr} - (d_{12}^{nr})^2/d_{11}^{nr} & 0 \\ 0 & 0 & 2(1+\nu_{23})d_{22}^{nr} \end{bmatrix} \times \begin{Bmatrix} \sigma_x(t_r) \\ \sigma_y(t_r) \\ \sigma_{xy}(t_r) \end{Bmatrix} + \begin{Bmatrix} \epsilon_x^*(t) \\ \epsilon_y^*(t) \\ 0 \end{Bmatrix} \tag{A.14}$$

and thermal expansion coefficients are

$$\alpha_{xx} \text{ and } \alpha_{yy} = \alpha_{22} + \nu_{12}\alpha_{11} \tag{A.15}$$

The form of Eq. (A11) or Eq. (A.14) can be converted to that of Eq. (20), in which stress is the dependent variable, by following the procedure described in Ref. [44].

References

[1] Chapman TJ, Gillespie JW, Pipes RB, Manson J-AE, Seferis JC. Prediction of process-induced residual stresses in thermoplastic composites. Journal of Composite Materials 1990;24:616–41.

[2] Kwon YW, Berner JM. Matrix damage of fibrous composites: effects of thermal residual stresses and layer sequences. Computers & Structures 1997;64(1–4):375–82.

[3] Gao S-L, Kim J-K. Cooling rate influences in carbon fibre/PEEK composites. Part 1. Crystallinity and interface adhesion. Composites: Part A: Applied Science and Manufacturing 2000;31:517–30.

[4] Talbott MF, Springer GS, Berglund LA. The Effects of crystallization on the mechanical properties of PEEK polymer and graphite fiber reinforced PEEK. Journal of Composite Materials 1987;21:1056–81.

[5] Davies P, Cantwell WJ, Jar PY, Richard H, Neville DJ, Kausch H. Cooling rate effects in carbon fiber/PEEK composites. In: Composite Materials: Fatigue and Fracture, ASTM STP 1110, 1991. p. 70–88.

[6] Cantwell WJ, Davies P, Kausch HH. The effect of cooling rate on deformation and fracture of IM6/PEEK Composites. Composite Structures 1990;14:151–71.

[7] Cantwell WJ, Kausch HH. An evaluation of the interlaminar fracture

toughness of a thermoplastic composite with offset center flies. Mekhanika Kompozitnykh Materialov 1992;4:476–83.
[8] Cebe P, Chung SY, Hong S-D. Effect of thermal history on mechanical properties of polyetheretherketone below the glass transition temperature. Journal of Applied Polymer Science 1987;33:487–503.
[9] Tregub A, Harel H, Marom G. The influence of the thermal history on the mechanical properties of poly(ether ether ketone) matrix composite materials. Composite Science and Technology 1993;48:185–90.
[10] Lawrence WE, Seferis JC, Gillespie JW. Material response of a semicrystalline thermoplastic polymer and composite in relation to process cooling history. Polymer Composites 1992;13(2):86–96.
[11] D'Amore A, Nicolais L. The effect of fibre and crystallinity content on the structural relaxation of polyetheretherketone (PEEK). Composites Manufacturing 1992;3:25–31.
[12] Unger WJ, Hansen JS. The effect of cooling rate and annealing on residual stress development in graphite fiber reinforced PEEK laminates. Journal of Composite Materials 1993;27(2):108–37.
[13] Gurtin ME, Murphy LF. On optimal temperature paths for thermorheologically simple viscoelastic materials. Quarterly of Applied Mathematics 1980;38:179–89.
[14] Weitsman Y. Optimal cool-down in linear viscoelasticity. ASME Journal of Applied Mechanics 1980;47:35–9.
[15] Weitsman Y, Harper BD. Optimal cooling of cross-ply composite laminates and adhesive joints. ASME Journal of Applied Mechanics 1982;49:735–9.
[16] Harper BD. Optimal cooling paths for a class of thermorheologically complex viscoelastic materials. ASME Journal of Applied Mechanics 1985;52:634–8.
[17] Lee K, Weitsman Y. Optimal cool down in nonlinear thermoviscoelasticity with application to graphite/PEEK (APC-2) laminates. ASME Journal of Applied Mechanics 1994;61:367–74.
[18] Weitsman Y, Zhu H. On the minimization of residual thermal stresses in viscoplastic materials. International Journal of Solids and Structures 1993;30(20):2813–7.
[19] Ersoy NB. Prediction and measurement of residual stresses in layered composites. PhD Dissertation, Boğaziçi University, Istanbul, 1998.
[20] Özısık MN. Heat conduction. New York: John Wiley and Sons, 1980.
[21] Avrami M. Kinetics of phase change. II, transformation-time relations for random distribution of nuclei. Journal of Chemical Physics 1940; 8:212–24.
[22] Kamal MR, Chu E. Isothermal and nonisothermal crystallization of polyethylene. Polymer Engineering and Science 1983;23(1):27–31.
[23] Velisaris CN, Seferis JC. Crystallization kinetics of polyetheretherketone (PEEK) matrices. Polymer Engineering and Science 1986; 26(22):1574–81.
[24] Velisaris CN, Seferis JC. Heat transfer effects on the processing-structure relationship of polyetheretherketone (PEEK) based composites. Polymer Engineering and Science 1988;28(9):583–91.
[25] Cebe P. Application of parallel avrami model to crystallization of poly(etheretherketone). Polymer Engineering and Science 1988; 28(18):1192–7.
[26] Cebe P. Non-isothermal crystallization of poly(etheretherketone) aromatic polymer composite. Polymer Composites 1988;9(4):271–9.
[27] Motz H, Schultz JM. The solidification of PEEK. Part I: morphology. Journal of Thermoplastic Composite Materials 1989;2:248–66.
[28] Eduljee RF, Gillespie JW, McCullough RL. Residual stress development in neat poly(etheretherkethone). Polymer Engineering and Science 1994;34(6):500–6.
[29] Wang T-M, Daniel IM, Gotro JT. Thermoviscoelastic analysis of residual stresses and warpage in composite laminates. Journal of Composite Materials 1992;26(6):883–99.
[30] Jeronimidis G, Parkyn AT. Residual stresses in carbon fibre–thermoplastic matrix laminates. Journal of Composite Materials 1988;22: 401–14.
[31] Kim K, Hahn HT, Croman RB. The effect of cooling rate on residual stresses in a thermoplastic composite. Journal of Composites, Technology and Research 1989;11(2):47–52.
[32] Li MC, Wu JJ, Loos AC, Morton J. A plane stress finite element model for process-induced residual stresses in a graphite/PEEK composite. Journal of Composite Materials 1997;31(3):212–43.
[33] Nejhad MNG, Gillespie JW, Cope RD. Prediction of process-induced stresses for in-situ thermoplastic filament winding of cylinders. In: Proceedings of 3rd International Conference of Computer Aided Design in Composite Material Technology, Newark, DE, 1992, Vol. 3, p. 277–295.
[34] Barnes JA. Thermal expansion behavior of thermoplastic composites. Journal of Material Science 1993;28:4974–82.
[35] Lawrence WE, Manson J-AE, Gillespie JW, Pipes RB. Prediction of residual stress in continuous fiber semicrystalline in thermoplastic composites: a kinetic viscoelastic approach. In: Proceedings of American Society for Composites Fifth Technical Conference, E. Lansing, MI, June 12–14, 1990. p. 401–14.
[36] Xiao XR. Characterization and modeling of nonlinear viscoelastic response of PEEK resin and PEEK composites. Composites Engineering 1994;4(7):681–702.
[37] Horoschenkoff A. characterization of the creep compliances J_{22} and J_{66} of orthotropic composites with PEEK and epoxy matrices using the nonlinear viscoelastic response of the neat resins. Journal of Composite Materials 1990;24:879–91.
[38] Morland LW, Lee EH. Stress analysis for linear viscoelastic materials with temperature variation. Transactions of the Society of Rheology 1960;4:233–63.
[39] Shapery RA. Stress analysis of viscoelastic composite materials. Composite Materials 1967;1:228–67.
[40] Christensen RM. Theory of viscoelasticity. Academic Press, New York, 1982.
[41] Yang TY. Finite element structural analysis. Prentice-Hall, Englewood Cliffs, NJ, 1986.
[42] Lynch FS. A finite element method of viscoelastic stress analysis with application to rolling contact problems. International Journal for Numerical Methods in Engineering 1969;1:379–94.
[43] Batra RC. Cold sheet rolling, the thermoviscoelastic problem. A numerical solution. International Journal for Numerical Methods in Engineering 1977;11:671–82.
[44] Sonmez FO, Hahn HT. Thermoviscoelastic analysis of the thermoplastic composite tape placement process. Journal of Thermoplastic Composite Materials 1997;10(4):381–414.
[45] Sonmez FO. Modeling of the thermoplastic composite tape placement process. PhD Dissertation, University of California, Los Angeles, 1995.
[46] Nelder JA, Mead R. A simplex method for function minimization. Computer Journal 1965;7(4):308–13.
[47] Cogswell FN. Thermoplastic aromatic polymer composites. Butterworth-Heinemann Ltd, Oxford, 1992.
[48] Making consolidated sheet from aromatic polymer composite APC-2, Data sheet 2, ICI Fiberite Corp., 1987.
[49] Grove SM. Thermal modelling of tape laying with continuous carbon-fiber-reinforced thermoplastics. Composites 1988;19:367–75.
[50] Blundell DJ, Willmouth FM. Crystalline morphology of the matrix of PEEK-carbon fiber aromatic polymer composites. SAMPE Quarterly 1986;17(2):50–7.
[51] Lee K, Weistman Y. Residual thermal stresses in graphite/PEEK (APC-2) laminates. In: Fujiwara H, Abe T, Tanaka K, editors. Residual stresses—III, London: Elsevier Science Publishers Ltd, 1992. p. 31–7.
[52] Barnes JA, Simms IJ, Farrow GJ, Jackson D, Wostenholm G, Yates B. Thermal expansion behavior of thermoplastic composite materials. Journal of Thermoplastic Composite Materials 1990;3:66–80.
[53] Manson JA, Seferis JC. Internal stress determination by process simulated laminates. In: SPE ANTEC 1987 Conference Proceedings, Los Angeles, CA.
[54] Ersoy N, Vardar O. Measurement of residual stresses in layered composites by compliance method. Journal of Composite Materials 2000;34(7):575–98.